*Physicochem. Probl. Miner. Process., 61(6), 2025, 216318*

http://www.journalssystem.com/ppmp

Physicochemical Problems of Mineral Processing

ISSN 1643-1049


# Process mineralogy of high-silicon iron tailings from Hebei province by MLA

**Yueshan Gao [1], Fusheng Niu [1,2], Jinxia Zhang [1,2], Chao Yang [1], Xinggeng Xie [1]**

[1] College of Mining Engineering, North China University of Science and Technology, Tangshan 063210, China

[2] Collaborative Innovation Center of Green Development and Ecological Restoration of Mineral Resources, Tangshan 063210, China

Corresponding author: kyky@ncst.edu.cn (Jinxia Zhang)

**Abstract:** Mineral liberation analyser (MLA) was applied to quantitatively analyze the High-Silicon iron tailings from Hebei Province. Mineralogy parameters, such as chemical composition, mineral composition, element occurrence state, mineral grain size distribution, mineral assemblage, and liberation degree. Results show that the iron grade in the iron tailings is 9.18%, and the silicon grade is 44.22%. Iron is primarily hosted in gangue minerals such as olivine (45.65%) and chlorite (20.19%), with lesser amounts present in metallic minerals like magnetite (12.11%). Silicon is predominantly hosted in quartz (59.90%), followed by silicate minerals such as plagioclase feldspar (19.46%). The iron-bearing mineral in the iron tailings is magnetite, with a content of 1.23%. The primary gangue minerals include quartz, sodium feldspar, potassium feldspar, olivine, and chlorite, among which quartz has the highest content at 41.23%. Iron tailings have a broad particle size distribution and poorly liberated minerals. The mineral intergrowth relationships are complex, featuring close intergrowths between different minerals. Magnetite often occurs as a gap-filling material between intergrown grains of quartz and silicate minerals, making it difficult to both liberate and recover. Quartz is a recyclable gangue mineral that often occurs closely intergrown with silicate minerals such as feldspar and olivine, forming irregular polygonal interlocking structures. Both its liberation and recovery are challenging. To recover quartz, tailings must undergo thorough liberation, while also addressing iron removal and the separation of quartz from silicate minerals like albite and potassium feldspar. The research findings provide fundamental theoretical data for the comprehensive recovery and utilization of iron tailings.

***Keywords:*** processing mineralogy, iron tailings, MLA, quartz

## 1. Introduction

With the rapid development of China's mining and steel industries, the demand for iron ore has increased year by year, leading to a significant rise in iron tailings discharge (Pan et al., 2018). Iron tailings in China are characterized by diverse types, complex compositions, and fine grain sizes (Yin et al., 2023). Due to variations in regional resources, the composition and content of iron tailings also differ. Iron tailings are chemically composed primarily of silicon, aluminum, calcium, and magnesium oxides, with minor amounts of potassium, sodium, iron, and sulfur oxides, exhibiting relatively high silicon and aluminum content (Xiao et al., 2010; Freitas et al., 2019). Unrecycled iron tailings are primarily disposed of in tailings dams, which not only wastes land resources but also poses severe environmental risks such as tailings dam failures, soil contamination, and dust storms, threatening the surrounding ecology and the safety of residents (Maass et al., 2019; Li et al., 2019; Luo et al., 2020). Statistics indicate that in 2024, China's annual production of iron tailings reached approximately 600 million tons, yet the comprehensive utilization rate remained below 40% (Wang et al., 2025). With the implementation and advancement of green development, promoting the comprehensive utilization of bulk industrial solid waste has become a crucial means for resource circulation and sustainable economic development (Sun et al., 2024; Hou et al., 2024; Niu et al., 2024). As a typical industrial solid waste resource, the rational

DOI: 10.37190/ppmp/216318

development and utilization of iron tailings holds profound significance for environmental protection and resource recycling.

In recent years, with continuous advancements in mineral processing technology and improvements in recovery processes for valuable components, the concentration of primary useful elements in iron tailings has gradually decreased. This has gradually transformed quartz gangue minerals into an underutilized secondary resource with significant economic value (Zhang et al., 2019; Lin et al., 2020; Liu et al., 2024). Against this backdrop, as China's demand for high-purity quartz continues to rise to support its advanced high-tech industries, researchers both domestically and internationally have increasingly proposed recovering high-purity quartz from iron tailings to replace the dwindling natural high-quality quartz mineral resources (Huang et al., 2020; Yang et al., 2017). However, research on the process mineralogical characteristics of typical high-silica iron tailings in Hebei Province remains relatively scarce, hindering the efficient comprehensive utilization of iron tailings resources.

With technological advancements and equipment upgrades, mineral detection methods continue to evolve. The Mineral Automatic Analyzer (MLA) represents a novel automated instrument for mineral analysis. Its principle combines BSE image analysis with X-ray mineral identification and computer software to perform microscopic operations and collect mineralogical data (Ying, 2003; Cardoso et al., 2019). It offers advantages such as accurate and reliable measurement parameters and convenient data processing, providing rapid and precise quantitative analysis for minerals (Fu et al., 2019). This system has been widely applied to determine and analyze key parameters such as mineral composition, occurrence characteristics, particle size distribution, and degree of liberation in ores including cassiterite (Hu et al., 2019), copper-molybdenum ore (Li et al., 2018), rare earth ore (Wang et al., 2018; Xu et al., 2019), associated silver ore (Wang et al., 2015), coal gangue (Li et al., 2018), and lead-zinc oxide ore (Fang et al., 2012).

This study focuses on high-silicon iron tailings from a mineral processing plant in Hebei Province. Utilizing Mineral Logos Analyzer (MLA), systematic process mineralogy research was conducted on the iron tailings to provide precise data analysis and theoretical support for their further comprehensive utilization.

## 2. Materials and methods

The iron tailings were obtained from a mineral processing plant in Hebei Province. The particle size of the ore sample was approximately 2-0 mm. After thorough mixing, it was used as the original sample. The MLA Mineral Automated Analyzer from FEI Australia comprises an FEI scanning electron microscope, an EDAX energy dispersive X-ray spectrometer, and MLA650 automated testing software for process mineralogy. The epoxy resin (C105-B), graphite (G67500), curing agent (C205-B), and polishing solution (C40-6633) required for sample preparation are all pure analytical grade products purchased from Fisher Scientific Company in Canada.

Take a 1.0 g subsample of iron tailings, mix it with epoxy resin and hardener, then add the mixture to a plastic mold. Mix thoroughly, heat, and allow to cure for 24 hours to obtain the MLA resin sample. The sample surfaces were subjected to further polishing using polishing solutions. After polishing, the samples were cleaned, dried, and coated with carbon. Mineral composition, target mineral grain size, degree of liberation, intergrowth patterns, and element occurrence states were determined using MLA analysis. Fig. 1 illustrates the process of determining iron tailings using the MLA mineral analyzer. Each color represents a distinct mineral, and various process mineralogical parameters can be obtained through computer data processing.

## 3. Results and discussion

### 3.1. Chemical composition and mineral composition of iron tailings

Chemical composition and mineralogical analysis of iron tailings from a mineral processing plant in Hebei Province were conducted. The chemical composition results are presented in Table 1, while the mineralogical composition results are shown in Table 2.

As shown in Table 1, the primary chemical elements in the ore sample are Si, Fe, O, Al, K, Mg, Ca, and Na, with minor amounts of S, Ti, P, Mn, Ce, and La. The Si content in this iron tailings sample is the highest at 44.22%, classifying it as a typical high-silica iron tailing (Yan et al., 2025).

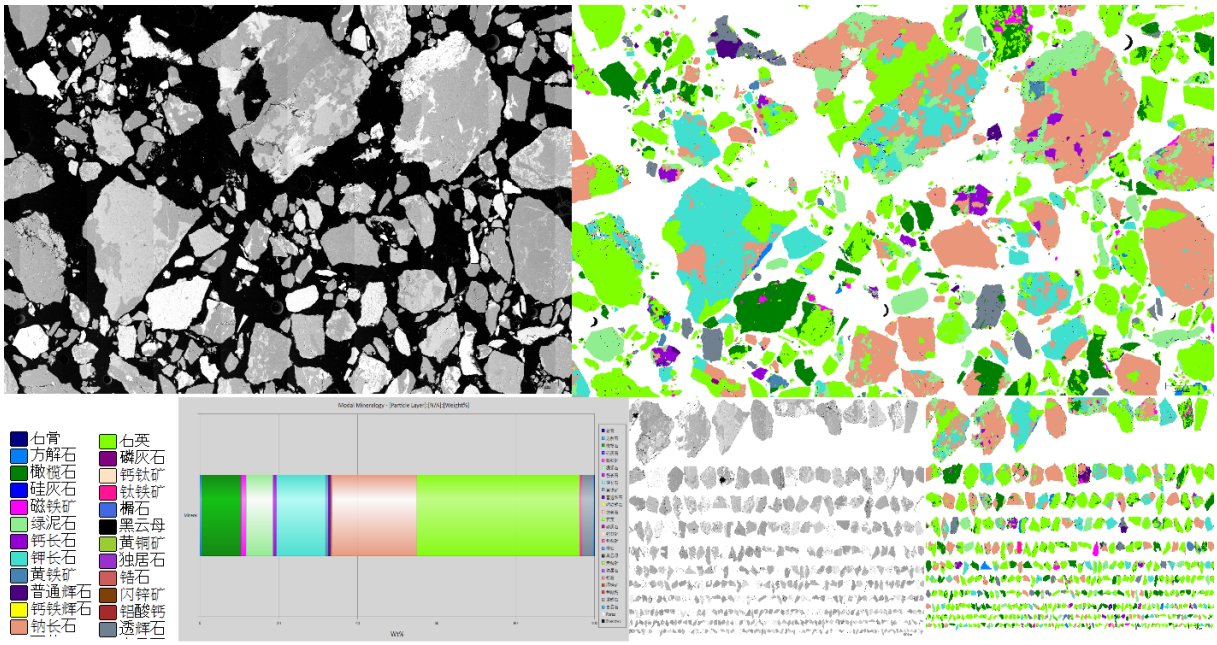


Fig. 1. The process of determining iron tailings with MLA mineral analyzer

Table 1. Multi-element analysis results of the ore (wt%)

| Element | Si | O | Fe | Al | K | Mg | Ca |
|---|---|---|---|---|---|---|---|
| Content | 44.22 | 31.58 | 9.18 | 5.92 | 3.14 | 2.04 | 1.99 |
| Element | Na | S | Ti | P | Mn | Ce | La |
| Content | 1.27 | 0.3 | 0.26 | 0.05 | 0.03 | 0.01 | 0.01 |

Table 2. Mineral composition and contents in the ore (wt%)

| Element | Quartz | Albite | Potassium feldspar | Olivine | Chlorite | Diopside | Magnetite |
|---|---|---|---|---|---|---|---|
| Content | 41.23 | 21.47 | 12.33 | 9.97 | 6.81 | 2.75 | 1.23 |
| Element | Anorthite | Augite | Pyrite | Calcite | Ilmenite | Dolomite | Hedenbergite |
| Content | 0.93 | 0.76 | 0.71 | 0.47 | 0.45 | 0.35 | 0.2 |
| Element | Apatite | Wollastonite | Monazite | Perovskite | Zircon | Titanite | |
| Content | 0.19 | 0.06 | 0.03 | 0.02 | 0.01 | 0.01 | |

As shown in Table 2. This iron tailings primarily contain quartz, albite, potassium feldspar, olivine, and chlorite. Among the silicate minerals, quartz (41.23%), albite (21.47%), and potassium feldspar (12.33%) dominate, with minor amounts of olivine, chlorite, pyroxene, and others. The iron tailings contain extremely low levels of magnetite, a valuable mineral, making their recovery economically unfeasible. However, they exhibit a high quartz content, which can serve as the primary recoverable mineral from these tailings. Experiments can be conducted to purify quartz from this iron tailings. Magnetic separation can be used to remove most magnetic minerals, while flotation can separate quartz from other silicate minerals.

### 3.2. Occurrence state of valuable elements in iron tailings

The distribution of valuable elements within ore is a critical factor determining its processing methodology. Analyzing the occurrence states of aluminum, iron, magnesium, and silicon in iron tailings using the MLA automatic mineral analyzer provides theoretical guidance for tailings processing. Table 3 presents the analysis of valuable element occurrence states in iron tailings.

Table 3. The distribution of elements in the ore (wt%)

| Mineral | Al | Fe | Mg | Si |
|---|---|---|---|---|
| Albite | 59.19 | - | - | 19.46 |
| Potassium Feldspar | 24.42 | 10.66 | - | 9.09 |
| Chlorite | 12.71 | 20.19 | 39.43 | 2.95 |
| Anorthite | 2.56 | - | - | 0.62 |
| Augite | 1 | 1.8 | 2.84 | 0.38 |
| Hedenbergite | 0.06 | 0.42 | 0.27 | 0.11 |
| Monazite | 0.03 | - | - | 0.01 |
| Wollastonite | 0.01 | 0.01 | 0.05 | 0.02 |
| Pyrite | 0.01 | 4.44 | 0.03 | 0 |
| Sphene | 0 | 0.01 | 0.01 | 0 |
| Olivine | 0 | 45.56 | 42.97 | 5.66 |
| Perovskite | - | 0.04 | - | 0 |
| Ilmenite | - | 2.02 | - | - |
| Magnetite | - | 12.11 | - | 0.01 |
| Quartz | - | - | - | 59.9 |
| Calcite | - | 0.02 | - | 0.01 |
| Zircon | - | - | - | 0.01 |
| Diopside | - | 2.21 | 12.72 | 1.77 |
| Dolomite | - | 0.49 | 1.68 | - |

As shown in Table 3, silicon is primarily present in gangue minerals such as quartz and feldspar, with quartz containing the highest proportion at 59.9%. Quartz is the sole natural raw material for industrial silicon production, while feldspar is not typically used as a silicon source. This is primarily because feldspar is a silicoaluminate mineral, where its silicon-oxygen tetrahedra and aluminum-oxygen tetrahedra are linked by cations such as potassium, sodium, and calcium. Its structure is more stable than quartz, requiring higher energy or stronger chemical reagents to disrupt its crystal lattice.

The occurrence state of iron is relatively complex, comprising silicate and oxide phases. It is primarily hosted in olivine, chlorite, magnetite, and potassium feldspar, with olivine containing the highest iron content at 45.56%. Over 70% of iron is present in gangue minerals, with only 20% occurring in magnetic minerals. Magnetic separation yields limited iron minerals, while iron from olivine can be extracted via pyrometallurgical and hydrometallurgical methods—though these processes suffer from high energy consumption and environmental pollution. How to achieve low-cost recovery of iron from olivine remains an open question.

Aluminum is primarily present in silicate minerals such as albite, potassium feldspar, chlorite, and anorthite. Albite contains the highest proportion of aluminum at 59.19%, followed by potassium feldspar and chlorite. Technically, it is feasible to extract aluminum from albite, but this process faces challenges such as high energy consumption, high chemical usage, and significant silicon slag pollution. Due to its poor economic viability and environmental impact, sodium feldspar is generally not considered a practical option for aluminum recovery.

Magnesium is primarily present in olivine, chlorite, diopside, and augite. Its highest concentration is found in olivine at 42.97%, followed by chlorite at 39.43%. Diopside also contains 12.72% magnesium. Based on the occurrence patterns of iron and aluminum elements, magnesium primarily forms layered and island-type silicates alongside iron and aluminum. Due to technological limitations, extracting magnesium from olivine is costly and yields minimal benefits, making it generally unfeasible to target olivine for magnesium recovery.

### 3.3. Particle size distribution of iron tailings and their primary minerals

To investigate the particle size distribution characteristics of major minerals in iron tailings, an automatic mineral analyzer system was employed to determine the particle size distribution of the iron

tailings and the particle size distribution of different mineral compositions. Mineral particle size distribution curves were plotted, with the results shown in Figs. 2 and 3.

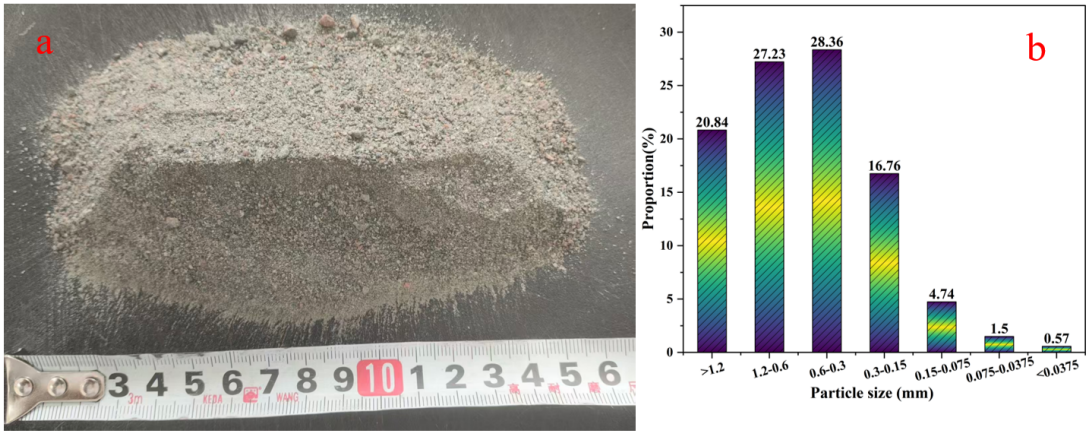


Fig. 2. (a) Appearance and (b) particle size distribution of the ore samples

As shown in Fig. 2, the iron tailings exhibit a grayish-white color, indicating a low TFe grade in the ore. Additionally, particle size analysis of the iron tailings indicates a broad particle size distribution dominated by coarse particles. The tailings are primarily concentrated within the +0.15 mm size fraction, with the -0.6+0.3 mm fraction exhibiting the highest proportion at 28.36%. -1.2+0.6 mm particle size fraction is the second most abundant, accounting for 27.23%. The iron tailings exhibit an uneven particle size distribution, with coarse particles relatively concentrated.

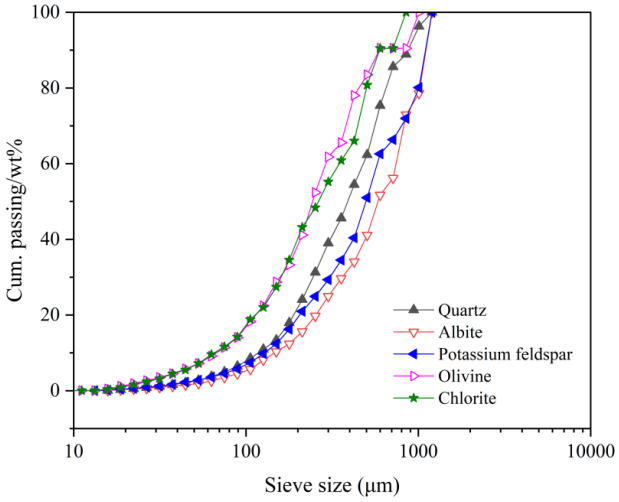


Fig. 3. Mineral grain size distribution

As shown in Fig. 3, olivine and chlorite particles are relatively fine, with 60% distributed between 0.01 and 0.15 mm. The albite and potassium feldspar grains are relatively coarse. Grains larger than 0.15 mm account for 89.65% and 87.61% of the sodium feldspar and potassium feldspar, respectively. The quartz content in iron tailings with particle sizes greater than 0.15 mm is 86.60%, slightly lower than that of albite and potassium feldspar. The iron tailings exhibit relatively coarse grain size distribution, necessitating further grinding to enhance quartz liberation and prepare for subsequent quartz purification.

### 3.4. Embedding characteristics of primary minerals in iron tailings

To investigate the mineral occurrence characteristics in iron tailings, an automated mineral analyzer system was employed to observe the liberation state and occurrence patterns of primary minerals in the tailings. The results are presented in Table 4 and Fig. 4.

Table 4. Intergrowth of main minerals (%)

| Mineral | Liberated | Association | | | |
|---|---|---|---|---|---|
| | | Albite | Potassium feldspar | Chlorite | Anorthite |
| Quartz | 41.48 | 8.59 | 10.4 | 5.01 | 0.23 |
| Albite | 14.78 | - | 16.5 | 23.27 | 3.21 |
| Potassium feldspar | 14.28 | 42.48 | - | 8.12 | 0.3 |
| Olivine | 41.37 | 5.69 | 1.22 | 2.38 | 0.67 |
| Anorthite | 11.05 | 43.13 | 3.42 | 20.35 | - |
| Mineral | Association | | | | |
| | Augite | Hedenbergite | Monazite | Wollastonite | Pyrite |
| Quartz | 0.31 | 0.55 | 0.02 | 0.12 | 0.23 |
| Albite | 1.37 | 0.3 | 0.11 | 0.16 | 0.79 |
| Potassium feldspar | 0.1 | 0.15 | 0.02 | 0.05 | 0.06 |
| Olivine | 0.17 | 0.93 | 0.06 | 0.05 | 0.66 |
| Anorthite | 4.77 | 0.24 | 0.37 | 0.03 | 0.36 |
| Mineral | Association | | | | |
| | Titanite | Olivine | Ilmenite | Magnetite | Apatite |
| Quartz | - | 17.69 | 0.09 | 5.65 | 0.37 |
| Albite | 0.01 | 3.48 | 0.04 | 0.5 | 0.54 |
| Potassium feldspar | - | 1.35 | 0.02 | 0.03 | 0.01 |
| Olivine | - | - | 0.17 | 2.08 | 0.09 |
| Anorthite | - | 8.52 | 0.08 | 0.13 | 0.57 |
| Mineral | Association | | | | |
| | Quartz | Calcite | Zircon | Diopside | Dolomite |
| Quartz | - | 1.87 | 0.01 | 3 | 0.22 |
| Albite | 30.57 | 0.03 | 0.04 | 0.16 | 0.01 |
| Potassium feldspar | 30.2 | 0.74 | 0.03 | 0.01 | - |
| Olivine | 40.85 | 0.19 | 0.01 | 2.12 | - |
| Anorthite | 6.9 | - | 0.06 | 0.01 | - |

As shown in Table 4, the MLA analysis of the intergrowth relationships among major minerals in iron tailings indicates relatively high degrees of liberation for quartz and olivine, at 41.48% and 41.37%, respectively; The degree of cleavage for potassium feldspar, Albite, and Anorthite is relatively low, at 14.28%, 14.78%, and 11.05%, respectively. Quartz that has not been completely liberated in the ore closely associates with nearly all minerals, most intimately with olivine, accounting for 17.69% of the total surface area. The silicate minerals that are not fully weathered−such as potassium feldspar, albite, and olivine—are closely interlocked with quartz. Quartz accounts for 30.2%, 30.57%, and 40.85% of the total surface area in these three minerals, respectively, followed by other silicate minerals.Among the primary minerals in iron tailings, quartz is most closely associated with magnetite, followed by olivine. Quartz and olivine collectively account for 5.56% and 2.08% of the total surface area, respectively. The association between chlorite and potassium feldspar and anorthite is also relatively close, with shared surface area ratios of 23.27% and 20.35% respectively. Most minerals exhibit complex intergrowth relationships and extremely poor liberation, necessitating optimized grinding regimens or combined processing techniques to enhance mineral liberation.

As shown in Fig. 4, the iron tailings exhibit complex mineral composition and diverse texture relationships. Quartz grains display irregular heteromorphic crystal structures, characterized by large size and continuous distribution, while olivine presents typical euhedral-subeuhedral crystal structures. Magnetite occurs as scattered or sparse disseminations, closely associated with quartz (Fig. 4(a)). Olivine pyroxene and common pyroxene both exhibit well-formed to sub-well-formed crystal structures and occur in close association (Fig. 4(b)). Quartz forms irregular polygonal interlocking structures with albite and potassium feldspar, exhibiting tortuous and tightly packed grain boundaries. Additionally, small amounts of chlorite are embedded within the sodium feldspar (Fig. 4(c)). Magnetite

occurs locally in patchy, mottled patterns, closely associated with olivine and quartz (Fig. 4(d)). Olivine forms a typical contiguous association with either albite or quartz, exhibiting straight, well-defined boundaries and close contact between the two minerals (Fig. 4(e)). Albite and augite interpenetrate and envelop each other, exhibiting a typical interwoven structure. Within this structure, albite and potassium feldspar come into direct contact along relatively straight boundaries, forming a characteristic contiguous intergrowth structure (Fig. 4(f)).

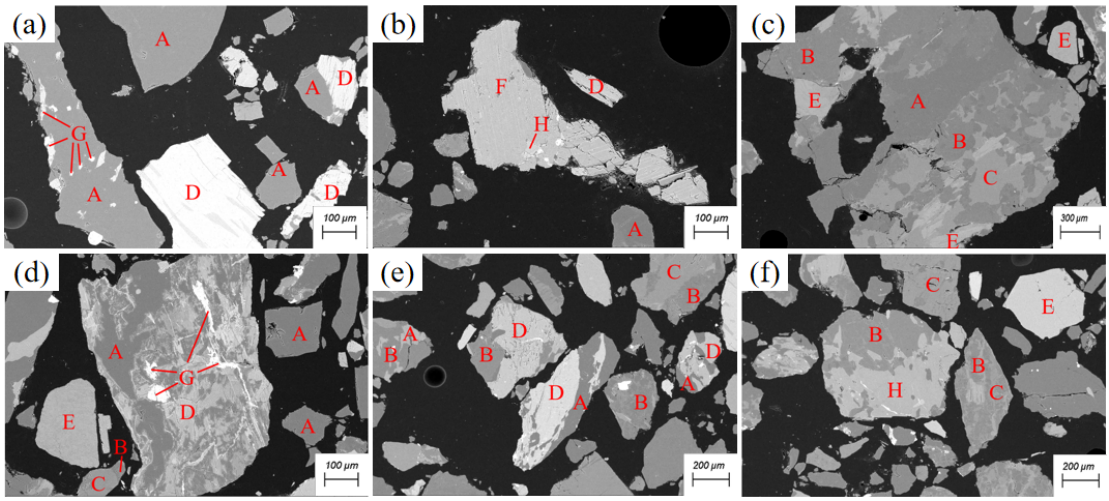


Fig. 4. MLA image of iron ore tailings. (A) Quartz; (B) Albite; (C) Potassium feldspar; (D) Olivine; (E) Chlorite; (F) Diopside; (G) Magnetite; (H) Augite

### 3.5. Monolithic dissociation degree and occurrence index of primary minerals

The free surface area of a mineral is defined as the percentage of surface area within a composite mineral particle that is not isolated or encapsulated by other minerals, thereby remaining accessible for external contact. The Mineral Occurrence Index (MOI) is a quantitative parameter generated by MLA software to describe the spatial distribution and aggregation degree of specific mineral phases within ore samples. It is defined as the ratio of the percentage of particle number frequency to the corresponding percentage of area fraction for the target mineral within a given measurement field of view. The quantification of this parameter was performed by the MLA system. Fig. 5 shows the cumulative distribution of minerals across different free surface area ranges in iron tailings, while Fig. 6 depicts the distribution characteristics of the quartz mineral occurrence index.

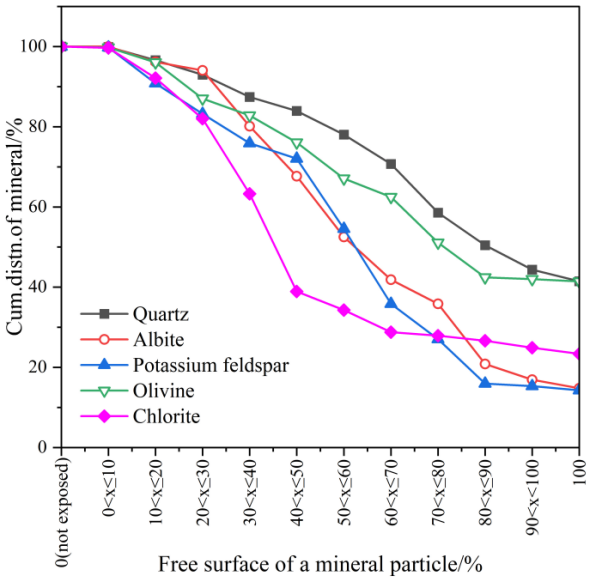


Fig. 5. Mineral liberation by free surface

As shown in Fig. 5, quartz and olivine exhibit relatively high degrees of liberation in iron tailings, while potassium feldspar, sodium feldspar, and chlorite demonstrate relatively low degrees of liberation. Among them, quartz exhibits the most gradual decline in curve, indicating that quartz predominantly exists as individual particles and can be separated through coarse grinding. The cleavage characteristics of albite and potassium feldspar are relatively similar, with their curves initially declining rapidly, indicating a greater tendency to form intergrowths with other minerals at medium grain sizes. The gradual decline in olivine's curve, second only to quartz's downward trend, indicates that olivine also predominantly exists as individual crystals and can be liberated through coarse grinding. The exfoliation behavior of chlorite indicates a low initial degree of exfoliation, which is closely related to the mineral's complex intergrowth relationships and its tendency to become muddy due to its low hardness. Chlorit readily generates secondary mineral slime during grinding, severely affecting subsequent mineral separation. This further illustrates that after determining the grinding regime, the ground product must undergo desliming treatment to minimize the impact of chlorite on the separation process.

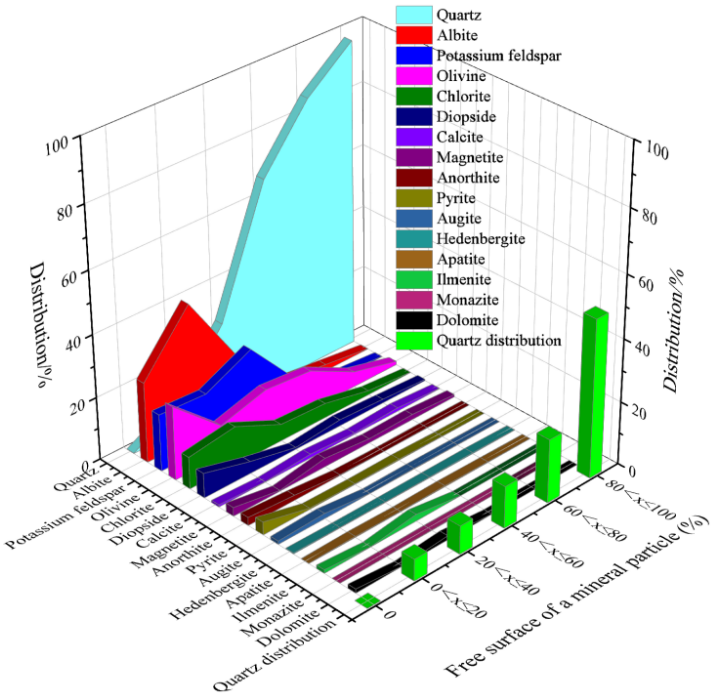


Fig. 6. Distribution of the mineral occurrence indicator (MOI) for quartz

As shown in Fig. 6, when the quartz liberation degree exceeds 80%, its distribution area proportion reaches 97.06%, indicating that quartz primarily exists as individual grains or high-grade intergrown bodies. Albite is primarily distributed within the ore matrix, with 25.61% of its distribution area occurring in the particle range completely devoid of quartz. Furthermore, it accounts for as much as 43.48% of the distribution in the range where quartz liberation is between 0 and 20%. Peridotite, potassium feldspar, and chlorite exhibit continuous distribution characteristics within the intermediate dissociation range (20%-80%) of quartz, forming complex heterogeneous structural relationships with quartz. Grinding treatment is required to enhance the individual liberation of quartz in iron tailings, thereby creating the necessary conditions for its subsequent efficient separation.

## 4. Recommendations for comprehensive utilization

### 4.1. Preparation of high-purity quartz based on flotation process

Based on the process mineralogical characteristics of iron tailings, a combined process flow of "grinding-magnetic separation-flotation-acid leaching" is recommended. The quartz in this iron tailings primarily occurs as coarse-grained inclusions with complex intergrowth relationships; An appropriate grinding regime must be established to ensure thorough liberation of the quartz. Magnetic separation

processes are employed to remove magnetic minerals from iron tailings, eliminating all magnetic impurities; Then, flotation is performed on the iron tailings to establish an appropriate reagent system; By activating non-magnetic impurities such as feldspar, the objective of enriching quartz is achieved; If the $SiO_2$ grade of the quartz concentrate obtained through flotation still fails to meet the quality requirements for high-purity quartz sand (≥ 99.90%), acid washing experiments using sulfuric acid, hydrochloric acid, or mixed acids must be conducted to further enhance the quartz $SiO_2$ grade. Technically speaking, further development of novel flotation reagents and processes with higher selectivity is required to enhance the separation efficiency of quartz and feldspar. LI et al studied high-silicon iron tailings from China (LI et al., 2023; LI et al., 2024). By employing superconducting high-gradient magnetic separation and high-temperature mixed acid leaching (fluorine-free) processes on iron tailings containing 81.39% $SiO_2$ and 15.21% $Fe_2O_3$, they obtained high-purity quartz with $SiO_2$ purity as high as 99.92%.

### 4.2. Resource utilization based on building materials

(1) Preparation of Autoclaved Aerated Concrete. Research indicates that iron tailings sand can serve as a siliceous raw material for producing autoclaved aerated concrete. Huang et al. (2024) successfully prepared high-silica iron tailings autoclaved aerated concrete using high-silica iron tailings as the sole siliceous raw material.

(2) Production of microcrystalline glass. This iron tailings can serve as the primary material for preparing pure black microcrystalline glass via the sintering method. Wang et al. (2020) successfully produced microcrystalline glass with a pure black color by using the $Al_2O_3$, $SiO_2$, CaO, and $Na_2O$ components from the iron tailings as the base constituents, adding iron oxide and cobalt oxide as colorants, and employing borax to adjust the gloss.

In summary, it is recommended that subsequent research pursue two parallel technical approaches: "flotation purification to obtain high-purity quartz" and "resource utilization for construction materials". This dual-track strategy aims to maximize the value and achieve high-value-added utilization of this iron tailings resource.

## 5. Conclusions

(1) The main conclusions of the study. A tailings sample from Hebei Province is dominated by Si, O, and Fe, with respective contents of 44.22%, 31.58%, and 9.18%. The sample consists primarily of gangue minerals, with minimal metal mineral content. The gangue minerals are primarily composed of quartz, feldspar, olivine, and chlorite, with residual amounts of metallic minerals consisting mainly of magnetite, pyrite, and ilmenite. Quartz has the highest relative content at 41.23%, followed by albite (21.47%), potassium feldspar (12.33%), olivine (9.97%), and chlorite (6.81%), among others.

(2) The iron tailings exhibit complex mineral distribution patterns, with significant particle size variations among different minerals. The gangue minerals, primarily quartz and feldspar, are predominantly coarse-grained and widely distributed; In contrast, metallic minerals such as magnetite and pyrite are mainly finely disseminated within the matrix of the main minerals, increasing the difficulty of liberating individual grains. The determination of mineralogical parameters indicates that quartz and olivine exhibit the highest distribution rates in the range where the degree of cleavage exceeds 60%, at 70.7% and 62.49% respectively. Albite, potassium feldspar, and chlorite demonstrate relatively poor cleavage. The most common and most extensive intergrowths occur between quartz and both albite and potassium feldspar.

(3) The elemental occurrence indicates that aluminum and magnesium are primarily enriched in silicate gangue minerals, while silicon is predominantly distributed in quartz (59.9%) followed by albite (19.46%). Small amounts of iron are enriched in magnetite (12.11%), pyrite (4.44%), and ilmenite (2.02%). This occurrence state indicates that a portion of iron can be removed through magnetic separation, while quartz and feldspar can be effectively separated and most of the silica enriched via flotation. Based on the process mineralogical characteristics of this iron tailings, it is recommended that subsequent mineral processing tests focus on selective grinding and efficient classification technologies, while developing targeted flotation reagents. This approach will provide a technical basis for achieving efficient utilization of iron tailings resources.

**Acknowledgments**

This research was funded by the Key Project of Hebei Natural Science Foundation (E2025209186), the Hebei Provincial Science and Technology Research and Development Platform Special Project (25363801D).

**References**

CARDOSO, C. E. D., ALMEIDA, J. C., LOPES, C. B., TRINDADE, T., VALE, C., PEREIRA, E., 2019. *Recovery of Rare Earth Elements by Carbon-Based Nanomaterials-A Review*. Nanomaterials, 9(6).

FANG, M. S., XIAO, Y. W., TONG, J. S., 2012. *Application of MLA on determining liberation degree and size of lead zinc oxide minerals*. Nonferrous Metals (Mineral Processing Section), 64(3), 1-3, 9.

FREITAS, V. A. A., BREDER, S. M., SILVAS, F. P. C., ROUSE, P. R., OLIVEIRA, L. C. A., 2019. *Use of iron ore tailing from tailing dam as catalyst in a Fenton-like process for methylene blue oxidation in continuous flow mode*. Chemosphere, 219, 328–334.

FU, Y., LI, Z., ZHOU, A., XIONG, S., YANG, C., 2019. *Evaluation of coal component liberation upon impact breakage by MLA*. Fuel, 258.

HOU, X., ZHANG, Y., LIU, X., et al., 2024. *Preparation and application of soil conditioner using iron ore tailings-biochar composite material*. Alexandria Engineering Journal, 94, 219-225.

HUANG, W., TANG, D., ZHANG, R. K., et al., 2024. *Autoclaved aerated concrete prepared with high-silicon iron tailing*. New Building Materials, 51(7), 1-5.

HUANG, Z., CHENG, C., LI, K., ZHANG, S., ZHOU, J., LUO, W., LIU, Z., QIN, W., WANG, H., HU, Y., HE, G., YU, X., QIU, T., FU, W., 2020. *Reverse flotation separation of quartz from phosphorite ore at low temperatures by using an emerging Gemini surfactant as the collector*. Separation and Purification Technology, 246, 116923.

HU, H. X., LI, G., 2019. *Application of MLA in study of characteristics and occurrences of porphyry tin ore in Guangdong province*. The Chinese Journal of Process Engineering, 19(1), 1-9.

LI, C., YANG, X. F., LI, Y. K., et al., 2024. *Preparation of high-purity $SiO_2$ by S-HGMS coupled with mixed-acid leaching: a case study on hematite tailings from Ansteel*, China. Waste Management, 174, 240-250.

LI, J. H., SUN, X. J., 2018. *Application of MLA technology in process mineralogy research on copper-molybdenum ore*. Nonferrous Metals (Mineral Processing Section), 70(5), 1-5.

LIN, M., LIU, Z., WEI, Y., LIU, B., MENG, Y., QIU, H., LEI, S., ZHANG, X., LI, Y., 2020. *A critical review on the mineralogy and processing for high-grade quartz. Mining*. Metallurgy & Exploration, 37(5), 1627-1639.

LI, R., ZHOU, Y., DUAN, X., 2019. *A novel composite phase change material with paraffin wax in tailings porous ceramics*. Applied Thermal Engineering, 151, 115-123.

LIU, Y., LIAO, C., LIU, L., et al., 2024. *Preparation of vanadium-titanium magnetite tailings/quartz sand monolithic composite and photocatalytic degradation of rhodamine B*. Minerals Engineering, 219, 108630.

LI, Y. K., LI, S. Q., ZHAO, X., et al., 2023. *Separation and purification of high-purity quartz from high-silicon iron ore tailing: an innovative strategy for comprehensive utilization of tailings resources*. Process Safety and Environmental Protection, 169, 142-148.

LI, Z., FU, Y. H., YANF, C., et al., 2018. *Mineral liberation analysis on coal components separated using typical comminution methods*. Minerals Engineering, 126, 74-81.

LUO, L., LI, K., FU, W., LIU, C., YANG, S., 2020. *Preparation, characteristics and mechanisms of the composite sintered bricks produced from shale, sewage sludge, coal gangue powder and iron ore tailings*. Construction and Building Materials, 232, 117250.

MAASS, D., VALÉRIO, A., LOURENÇO, L. A., OLIVEIRA, D., HOTZA, D., 2019. *Biosynthesis of iron oxide nanoparticles from mineral coal tailings in a stirred tank reactor*. Hydrometallurgy, 184, 199-205.

NIU, F., CHEN, Y., ZHANG, J., LIU, F., WANG, Z., 2024. *Selective flocculation-flotation of ultrafine hematite from clay minerals under asynchronous flocculation regulation*. International Journal of Mining Science and Technology, 34(11), 1563-1574.

PAN, D. A., LU, H. Y., LIU, X. M., et al., 2019. *Research progress and prospect on utilization of iron tailings for building materials*. Bulletin of the Chinese Ceramic Society, 38(10), 3162-3169, 3214.

SUN, X., MA, Y. W., YAO, F. X., et al., 2024. *Research progress on preparation of mineral materials from iron tailings*. Mining Research and Development, 44(9), 252-262.

WANG, J. P., WU, H. M., WANG, L., 2015. Application of MLA in the study of silver occurrence status. Mining & Metallurgy, 24(1), 77-80.

WANG, M., 2020. *Overview of the preparation process of black glass-ceramics from iron tailings*. Modern Mining, 36(6), 252-254.

WANG, X. T., HUA, S. G., PEI, D. J., et al., 2025. *Control and Comprehensive Utilization of Iron Tailings: Current Situation and Future Perspectives in China*. Metal Mine, (7), 243-253.

WANG, Y., HU, B. Q., LI, Y. G., et al., 2018. *Study of EMPA and MLA of associated rare earth in Zoujiashan uranium ore*. Chinese Rare Earths, 39(3), 17-26.

XIAO, L. G., YI, J. H., CUI, Z. X., 2010. *Iron tailings comprehensive utilization at home and abroad*. Journal of Jilin Institute of Architecture and Civil Engineering, 27(4), 22-26.

XU, C. L., ZHONG, C. B., LU, R. L., et al., 2019. *Process mineralogy of Weishan rare earth ore by MLA*. Journal of Rare Earths, 37(3), 334-338.

YANG, C., LI, S., ZHANG, C., BAI, J., GUO, Z., 2017. *Application of superconducting high gradient magnetic separation technology on silica extraction from iron ore beneficiation tailings*. Mineral Processing and Extractive Metallurgy Review, 39(1), 44-49.

YAN, H., GAO, Z. K., CHAO, X. L., et al., 2025. *Research Progress and Performance Evaluation of Asphalt Mixture*. Metal Mine, (8), 272-280.

YIN, C., BAI, L. M., LI, S. Y., et al., 2023. *Research progress of comprehensive utilization of iron tailings*. Conservation and Utilization of Mineral Resources, 43(4), 41-53.

YING, G.,2003. *Automated scanning electron microscope based mineral liberation analysis*. Journal of Minerals, Materials Characterization and Engineering, 2(1), 33-41.

ZHANG, X., HAN, Y., SUN, Y., LV, Y., LI, Y., TANG, Z., 2019. *An Novel Method for Iron Recovery from Iron Ore Tailings with Pre-Concentration Followed by Magnetization Roasting and Magnetic Separation*. Mineral Processing and Extractive Metallurgy Review, 41(2), 117-129.